



Assessment of the Effectiveness of Water Hyacinth (*E. crassipes*) in the Biosorption of Heavy Metals from Aluminium Extruding Company Effluents

FUBARA, AG; UCHE, CC; *NWOKO, CO, TONY-NJOKU, RF, OJIAKU, AA AND EDO, FA

Department of Environmental Management, Federal University of Technology, Owerri, Nigeria.
*Corresponding Author Email: conwoko2002@yahoo.com

ABSTRACT: Biosorption technique was used to assess the effectiveness of water hyacinth in the removal of heavy metal from effluents obtained from an Aluminium extruding company. Fourier transform infrared (FTIR) spectroscopy and scanning electron microscopy (SEM) techniques were used to characterize the water hyacinth materials before and after adsorption. A batch experiment was set up using water hyacinth (*E. crassipes*) ash as adsorbent. The effects of contact time, adsorbent dose, pH and temperature on the heavy metal removal efficiency were determined. The experimental data were analysed by the Langmuir, Freundlich and Temkin models of adsorption. The FTIR results showed a reduction in the intensity of the adsorption bands for all the metal ions. The optimal percentage removal of the metal occurred at 30 minutes except Cd which had highest percentage removal at 20 minutes while optimal pH was at 6.0 except Pb which had its optimal removal at pH 4.0. Increase in biosorbent dosage increased the percentage removal of the metal ions with Zn (96% at 1.0 g) having the highest percentage removal of the five metal ions studied. The results revealed that Langmuir and Temkin Isotherms were the best model for the metal ions adsorption onto water hyacinth. Langmuir model had a better fit for Fe ($R^2 = 0.78$), Ni ($R^2 = 0.82$) and Pb ($R^2 = 0.78$), while Temkin model fitted best for Cd ($R^2 = 0.92$) and Zn ($R^2 = 0.96$). The *E. crassipes*, therefore, could serve as effective, low-cost and environmentally friendly adsorbents.

DOI: <https://dx.doi.org/10.4314/jasem.v26i1.6>

Open Access Article: (<https://pkp.sfu.ca/ojs/>) This an open access article distributed under the Creative Commons Attribution License (CCL), which permits unrestricted use, distribution, and reproduction in any medium, provided the original work is properly cited.

Impact factor: <http://sjifactor.com/passport.php?id=21082>

Google Analytics: <https://www.ajol.info/stats/bdf07303d34706088ffffbc8a92c9c1491b12470>

Copyright: Copyright © 2022 Fubara *et al.*

Dates: Received: 23 August 2021; Revised: 21 December 2021; Accepted: 06 January 2022

Keywords: Water hyacinth, Biosorbent, Heavy metal, Fourier transform infrared, Scanning Electron Microscopy

Heavy metals in the environment have become a major threat to plants, animals, and human life due to their bio-accumulating tendency and toxicity and therefore must be removed from municipal and industrial effluents before being discharged (Horsfall *et al.*, 2005). Industrial effluents in developing economics are often released into the water bodies without taking care of the inorganic components or pollutants embedded in most waste water (Horsfall *et al.*, 2006). Biosorption is a physicochemical process that occurs naturally in certain biomass which allows contaminants to passively concentrate and bind on to the biomass cellular structure (Volesky, 1990). This phenomenon provides an economic alternative for removing heavy metals from industries waste water and aid in environmental remediation. Biosorption uses biomass raw materials which are either abundant (seaweeds) or wastes from other industrial operations

(fermentation waste). The major advantages of biosorption over the conventional treatment methods of waste water such as chemical precipitation, coagulation, flocculation, magnetic separation, membrane filtration, electro-dialysis, ion – exchange, electrochemical deposition etc., (Gunatilake, 2015) include; low cost, high efficiency, minimization of chemical and biological sludge, no additional nutrients requirement, regeneration of biosorbent and possibility of metal recovery. Environmentally, biosorption offers environmental friendly filtering, rigorous filtering of harmful pollutants created by industrial process and all round human activity. Recently, water hyacinth (*E. Crassipes*), has attracted significant attention as a sorbent material and this has been investigated by many authors (Mahamadi and Nharingo, 2007; Mahamadi and Nharingo, 2010). Uka *et al.* (2007) noted that water hyacinth (*E. Crassipes*)

*Corresponding Author Email: conwoko2002@yahoo.com

has high rate of invasion and colonization among other aquatic plants. *E. Crassipes* is alien to Nigerian aquatic ecosystem. The weed was first observed in 1984 (Akinyemiju, 1987) along Badagry Creek, from there it spreads through the entire coastline causing serious problem especially in fishing and transportation. However, the same plant has demonstrated an amazing ability to absorb and concentrate many toxic metals from aquatic environments (Mahamadi, 2011). The gradual proliferation of smelting and metal recycling industries in Nigeria is a threat to human life especially when the untreated effluents are discharged to the river courses and to arable land. These heavy metals are non-biodegradable but can easily find their way into the food chain thereby posing serious ecological risk

(He *et al.*, 2015). The major concern is to contain and remove heavy metals from the waste water effluents of these industries before discharge. The aim of the study was to assess the effectiveness of Water Hyacinth (*E. Crassipes*) as absorbent for heavy metal removal from an Aluminum recycling/extruding industry effluent.

MATERIALS AND METHODS

The raw waste water was obtained from Aluminum Extrusion Industry Plc (ALEX) situated about 4 km along the Atta Amaimo Road in Inyishi Village (Figure 1).

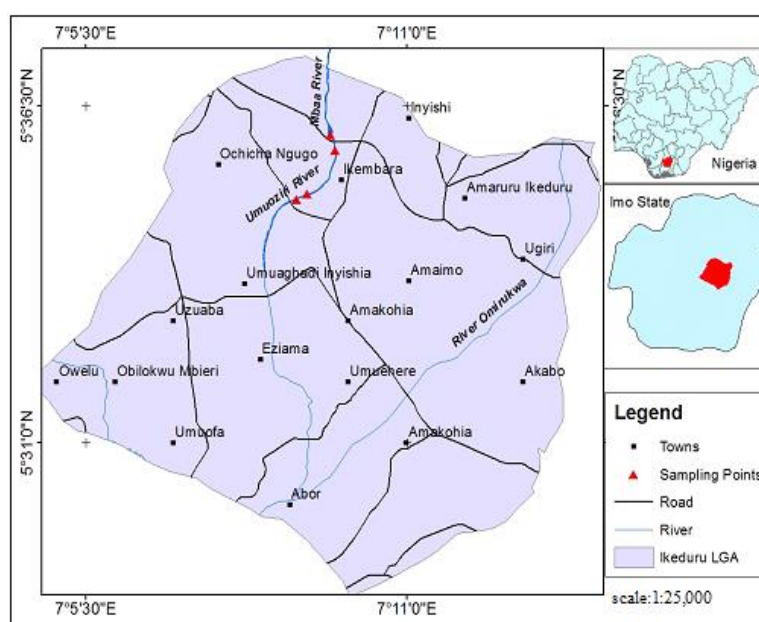


Fig 1: Map of Imo State, Nigeria, showing the study area

Sample collection and preparation: The Water Hyacinth was harvested from *Nwaorie* River, along ware-house road, Owerri, Imo State. It was washed with fresh water on site and packed for further treatment in the laboratory. The Water Hyacinth leaves were washed with distilled water and sun dried for 24 hours. Four hundred (400) g of the sample was weighed and introduced into a Muffle furnace at 400 °C for 30 minutes. This was allowed to cool and was then pulverized using a mortar and pestle.

Activation process: Water hyacinth was carbonized according to the method described by Abechi *et al.* (2013) with slight modification. 50 g carbonized sample was mixed with 0.5 M phosphoric acid and allowed to soak overnight, and then heated to form a paste. The sample was dried at 120 °C, the dried sample was then pyrolysed at a predetermined

temperature of 250 °C and activation time of 30 minutes in the furnace. The activated carbon was washed with de-ionized water repeatedly until the washing solution attained pH of 7.0. The prepared activated carbon was dried at 120 °C overnight, cooled and sieved through a 300 – 425 µm mesh. This was stored in a sealed plastic container for further processing.

Waste water digestion: The effluent was digested by introducing 50 mL of the effluent in a 250 mL conical flask and adding 10 mL of Aqua Regia composed of hydrochloric acid and nitric acid (3:1) and then heated on a hot plate until a volume of about 7-12 mL was left. The digest was filtered using Whatman No 42 filter paper and volume made up to 50 mL volumetric flask and stored for Atomic Absorption Spectrophotometer (AAS) analysis.

FUBARA, AG; UCHE, CC; NWOKO, CO, TONY-NJOKU, RF, OJIAKU, AA AND EDO, FA

Sample characterization: The chemical composition of the dried water hyacinth leaves was characterized using FTIR, and surface morphology analysed using scanning electron microscopy (SEM). FTIR spectra were recorded from 400 to 4,000 cm^{-1} using Perkin Elmer 400 FT-IR spectrophotometer. The concentrations of the metal ions of interest in the solutions before and after adsorption were determined using atomic absorption spectrophotometer AAS (Varian 710 ES model). The samples were filtered using 0.45 μm filter paper prior to analysis in order to obtain a clear solution and also to minimize interference of the biosorbent with the analysis.

Adsorption studies: The batch adsorption technique was employed to study the effect of adsorption dose, contact time, and temperature with the activated Water hyacinth. The experiment was carried out at ambient temperature (30 $^{\circ}\text{C}$) on an Erlenmeyer flasks placed on an orbital shaker for 50 minutes. The amount of pollutant adsorbed was calculated as:

$$\text{Adsorption capacity} = \frac{V(C_o - C_e)}{M} \quad (\text{i})$$

Where C_o and C_e (mg/L) are the initial and the equilibrium concentrations of the pollutant before and after adsorption process, and M (g) is the mass of the adsorbent, V (mL) is the volume of the raw waste water used for adsorption. The percentage pollutant removal was calculated using the equation:

$$\% \text{ Removal} = \frac{(C_o - C_e)}{C_o} \times 100 \quad (\text{ii})$$

Effect of adsorbent dose on biosorption: The effect of adsorbent dose was studied by varying the dosage used for adsorption. The dosages (g) of interest were 0.2, 0.4, 0.6, 0.8, and 1.0. The experiment was carried out by measuring 50 mL of the raw waste water into a 250 mL conical flask and the required adsorbent dose was introduced into the conical flask. The flask was agitated for 20 minutes at 350 rpm and 30 $^{\circ}\text{C}$. The mixture was filtered using a Whatman (0.45 μm) filter

paper. The filtrate analysed for unabsorbed heavy metal using AAS.

Effect of contact time on biosorption: The effect of contact time was studied by varying the agitation time. The samples were stirred for 10, 20, 30, 40 and 50 minutes using an orbital shaker. The experiment was carried out by measuring 50 mL of the raw waste water into a 250 mL conical flask and the optimum adsorbent dose was transferred into this conical flask and agitated for the specified time at 350 rpm and temperature of 30 $^{\circ}\text{C}$. The mixture was filtered using a Whatman (0.45 μm) filter paper. The filtrate was used for analysis of the pollutants remaining in the water using AAS.

Effect of temperature on biosorption: The reaction temperatures (30, 40, 50, 60 and 70 $^{\circ}\text{C}$) at optimized conditions of adsorbent dose and contact time were varied to determine the effect of temperature on water hyacinth adsorption. The mixture was filtered using a Whatman (0.45 μm) filter paper and the filtrate analysed for unabsorbed heavy metal.

Statistical Analysis: The data obtained were analyzed using descriptive statistics and results are presented in figures and tables.

RESULTS AND DISCUSSION

Biosorbent characterization using Fourier transform-Infra-Red Spectroscopy (FTIR): The FTIR analysis was done in order to study the possible adsorbent-metal interaction and identify the binding sites of the heavy metal adsorption available on the biosorbent. The spectra obtained were used to elucidate the mechanism of interaction between the metal cations in solution and the adsorbent (Figure 2). **Water Hyacinth morphology study:** Scanning electron microscope was done to determine the surface morphology of the biosorbent. This actually displays the surface profile of the adsorbent, and the pores of the biosorbent. Figure 3 display the SEM micrograph of the material before and after biosorption.

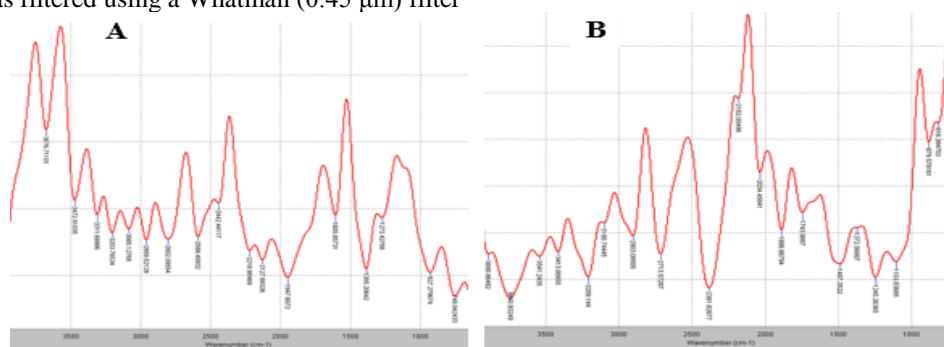


Fig 2: FTIR spectra of Water Hyacinth (A) before and (B) after adsorption studies

FUBARA, AG; UCHE, CC; NWOKO, CO, TONY-NJOKU, RF, OJIAKU, AA AND EDO, FA

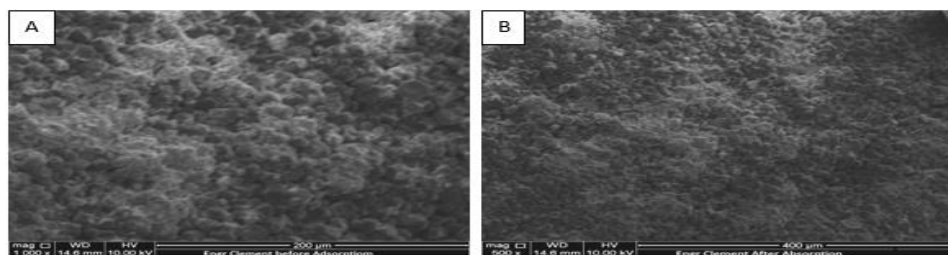


Fig 3: Scanning electron micrographs of water hyacinth (a) before and (b) after adsorption

FT-IR spectra of *E. Crassipes* (water Hyacinth) before and after adsorption (Figure 1) displayed a number of adsorption peaks indicating the complex nature of the examined adsorbent. The strong and broad peaks ranging from 3000 cm^{-1} - 3700 cm^{-1} represent the overlapping hydroxyl, phenols, amines, carboxylic acids and aromatics stretching vibrations. The peak observed at 2959.52 cm^{-1} is assigned to N-H stretch of amines and the strong and broad peak ranging from $2690\text{--}2840\text{ cm}^{-1}$ is assigned to the aldehydes and the ketones. The strong peak at 1605.85 cm^{-1} and 1385.20 cm^{-1} were assigned to the N-H bend of primary amines and S=O stretching of sulfate. The peaks at 927.27 cm^{-1} and 749.04 cm^{-1} were assigned to O-H bend of carboxylic acids and C-Cl stretch of alkyl halides (Munene *et al.*, 2020). From the spectra, it was observed that the intensity of the heavy metal loaded *E. Crassipes* was lower than the spectra of the *E. Crassipes* before adsorption and there was some shift or disappearance of the wave numbers after adsorption. For instance, the wave number appearing at 3676.71 cm^{-1} shifted to 3890.86 cm^{-1} . This shift suggests a chemical interaction between the free hydroxyl (O-H), phenols or amine groups and the metal cations (Ali and Hassaan, 2017). The primary amines and the alkyl halide groups also took part in the metal adsorption as their wave numbers shifted from 1605.85 cm^{-1} to 1743.98 cm^{-1} for the primary amines

and 1385.20 cm^{-1} to 1743.98 cm^{-1} for the alkyl halide groups, respectively after the metal adsorptions. These evidences from FT-IR spectroscopy points toward

complexation as the mechanism of adsorption by the Water hyacinth adsorbent. The metal cations bind themselves to the negatively charged -OH, -NH, -COO- and S=O binding sites. Figure 3 shows the SEM micrographs of the Water Hyacinth (*E. Crassipes*) samples before and after metal adsorption. The *E. Crassipes* exhibits granular-like, uneven and rough surface morphology. The pore of the adsorbent is noticed. However, the surface of the metal loaded adsorbent appear to be covered or coated with deposits of metal ion appearing as fine particles, hence reducing the pore sizes of the adsorbent after adsorption. Table 1.0 presents the result of the analysis of the raw ALEX effluent. From the result, it could be observed that Aluminium, Chromium and Cobalt were not detected in the company's effluent stream. The comparison of the raw effluent's metal concentrations with WHO standard shows that Zinc is about 8000% above WHO standard while Nickel, Lead and Cadmium were 89, 99 and 96% above WHO standard for drinking water. However, Iron (0.219 mg/L) and copper (0.063 mg/L) concentrations in the effluent were below WHO standard (2.0 mg/L in each case). Upon these findings, the five heavy metals (Nickel, zinc, Iron, Lead, and Cadmium) with the highest concentrations were selected for the biosorption experiment.

Characterization of waste water effluent: Table 1 presents the heavy metals composition of the raw effluent from the ALEX and their concentrations (mg/L) as compared to the WHO standard for drinking water (WHO, 2011).

Table 1. Heavy Metal content of raw waste water effluent

S/N	Parameters (mg/L)	ALEX effluent (mg/L)	WHO standard(mg/L)	Difference (%)
1	Copper	0.063 ± 0.02	2.000	(3075)
2	Iron	0.219 ± 0.01	2.000	(813)
3	Aluminium	ND	0.100	NA
4	Chromium	ND	0.050	NA
5	Cadmium	0.084 ± 0.01	0.003	96
6	Cobalt	ND	-	-
7	Nickel	0.622 ± 0.02	0.070	89
8	Zinc	4.070 ± 0.3	0.050	8040
9	Lead	0.779 ± 0.01	0.010	99
10	Arsenic	0.04 ± 0.01	0.010	(150)

Numbers in bracket signifies that ALEX effluent is less than WHO standard

Equilibrium sorption studies: One of the critical factors that influence adsorption of metal ion is pH. The pH of a solution directly affects the metal solubility or the dissociation degree of functional group located on the surface of adsorbent. An increase in pH means a lower amount of protons, which causes a decrease in the competition between protons and heavy metal ions. Increased pH is an indication that the ligands are available for metal ion binding, therefore, biosorption is enhanced (Ali *et al.*, 2014). Figure 4 shows the effects of pH on the adsorption of heavy metals from the ALEX effluent. The data showed that the adsorption of all the five metal ions increased as the pH increased. Lead was optimally adsorbed at pH 4 (acidic environment) while zinc, cadmium, nickel and iron adsorption peaked at pH 6. The decreased removal efficiency of all the five metal ions at low pH could have resulted from the increased positive charge on the surface of the biosorbents which causes electrostatic repulsion of the metal ions. As the pH increased, there resulted decreased competition between the metal ions and the H⁺ for the active sites of the *E. crassipes* adsorbent (Onwordi *et al.*, 2019). This result corroborates the study of Guyo and Moyo (2017) who reported a pH of 6 as the optimal for adsorption using treated cowpea pod. The optimal contact time for the adsorption of all the metal ions in this study occurred between 20 - 30 minutes of the investigation. The optimal percentage removal for Nickel, Iron, Lead and zinc occurred at 30 minutes with values of 92%, 88%, 83% and 82%, respectively while Cadmium attained equilibrium at 20 minutes of contact time with 88% removal. This results agrees with studies of Mahamadi and Nharingo (2010). Figure 6 presents the effect of temperature on the adsorption of heavy metals by *E. crassipes* (water hyacinth). Temperature has a vital effect on the adsorption process as it can influence the process by an increase or decrease in the amount of heavy metal adsorption. From the figure, it is shown that an increase in temperature increased adsorption. The uptake of Nickel, zinc, Iron, cadmium and lead ions increased as temperature increased similar to the reports by Genoveva *et al.* (2014), Ali *et al.* (2014) and Nwoko *et al.* (2016).

The optimal temperature in this study were between 40 - 50 °C. Zinc, Iron, Cadmium and Lead ions showed equilibrium percentage removal at 40 °C with values of 48, 44, 85 and 44%, respectively while Nickel, attained optimal percentage removal of 76% at 50 °C. This implied that Zinc, Iron, Lead and Cadmium were adsorbed to the biosorbent rapidly within the given temperature range.

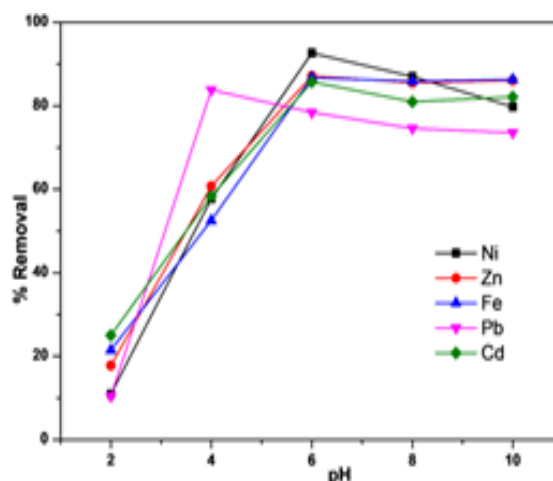


Fig 4: Effect of pH on the percentage removal of the studied metal ions onto *E. Crassipes* biosorbent.

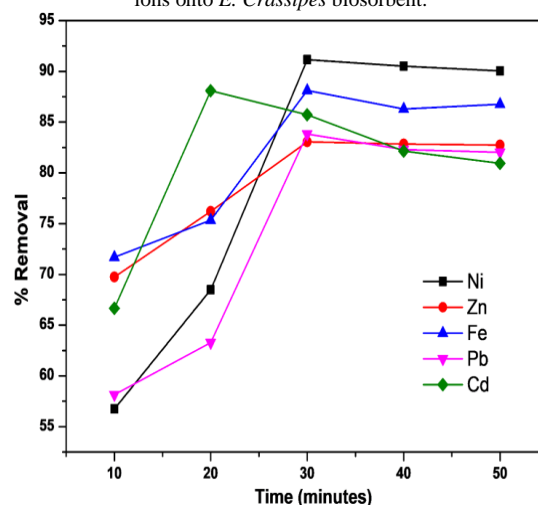


Fig 5: Effect of time on the percentage removal of the studied metal ions onto *E. crassipes* biosorbent.

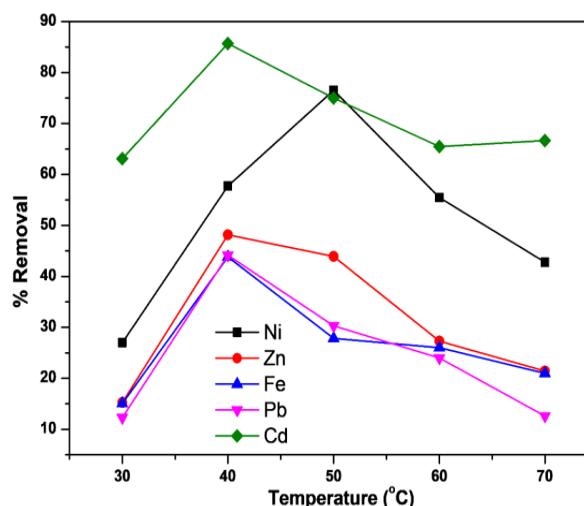


Fig 6: Effect of temperature on the percentage removal of the studied metal ions onto *E. crassipes* biosorbent.

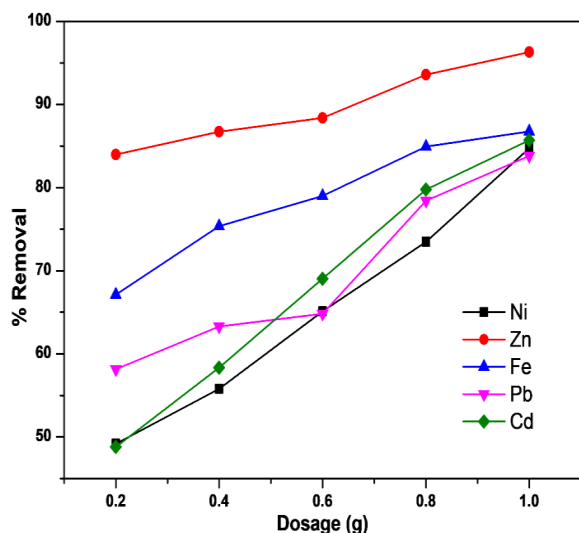


Fig 7: Effect of dosage on the percentage removal of the studied metal ions onto *E. crassipes* biosorbent.

Figure 7 presents the effect of adsorbent dosage on the uptake of heavy metals from the waste water effluent. It indicates that increase in the adsorbents' dosage from 0.2 – 1.0 g increased the percentage removal of the metal ions. The removal increased from 49 – 84%, 49 – 85%, 58 – 83%, 67 – 87% and 84 – 96% for Nickel, Cadmium, Lead, Iron and Zinc, respectively. The increase in adsorption with adsorbent dose could have resulted from the increased adsorbent surface area and the availability of additional adsorption sites on the biosorbent's surface (Shaban *et al.*, 2018).

Adsorption isotherms models: Adsorption is usually described through Isotherms, which relate to the amount of adsorbate on the adsorbent. Distribution of metal ions between the liquid phase and the solid phase can be described by several Isotherm models. The isotherm results were analyzed using Langmuir, Freundlich, and Temkin models. In each case, linear plots were obtained, which reveal the applicability of these isotherms on the adsorption study. Figure 8, 9 and 10 show Langmuir, Freundlich and Temkin plots, respectively for the adsorption of the five studied metal ions. The model parameters derived from these plot and correlation coefficients (R^2) are presented in Table 2. The correlation coefficient values obtained from the linear plot of the model was used to assess the applicability of the model to the adsorption process.

Langmuir isotherm: For the Langmuir adsorption model, Figure 8, the linearized equation was used. The linearized plot of specific adsorption ($1/q_e$), against the specific equilibrium concentration, ($1/C_e$), shows that the adsorption obeys the Langmuir model. The Langmuir constant Q_m and b were determined from the

slope and the intercept of the plot and are presented in Table 2.

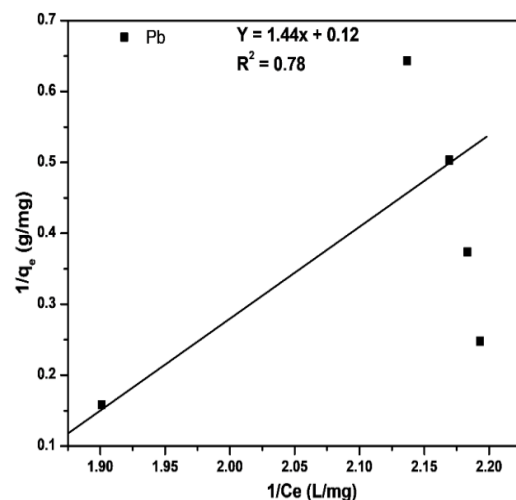


Fig 8a: Linear plots of Langmuir Isotherms for the adsorption of Pb, ions onto *E. Crassipes* biosorbents.

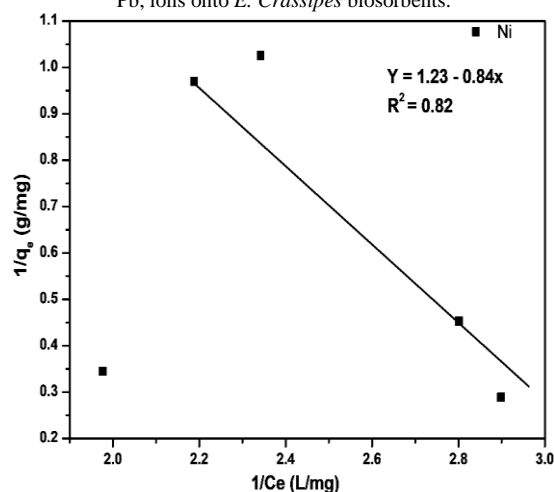


Fig 8b: Linear plots of Langmuir Isotherms for the adsorption of Ni ions onto *E. Crassipes* biosorbents.

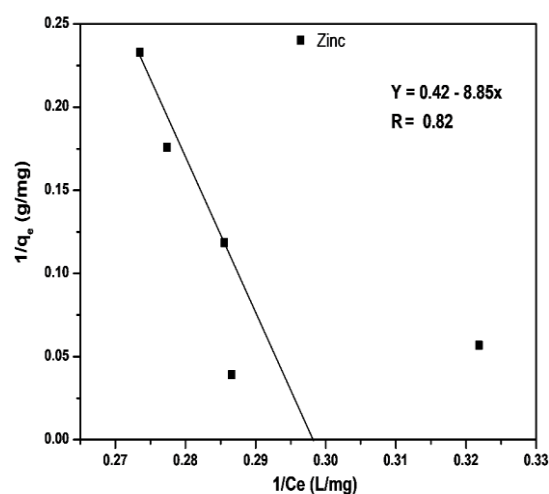


Fig 8c: Linear plots of Langmuir Isotherms for the adsorption of Zn ions onto *E. Crassipes* biosorbents.

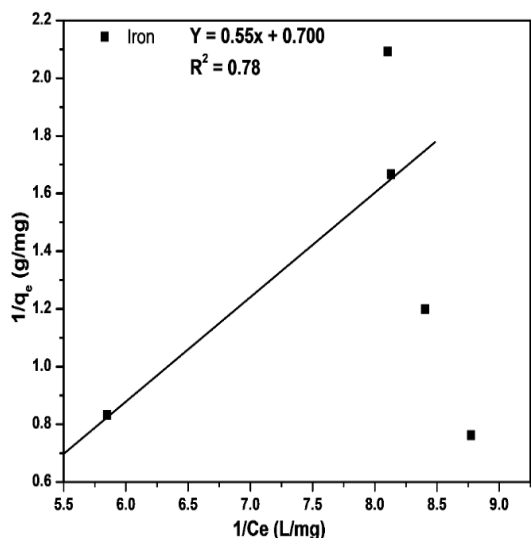


Fig 8d: Linear plots of Langmuir Isotherms for the adsorption of Fe ions onto *E. Crassipes* biosorbents.

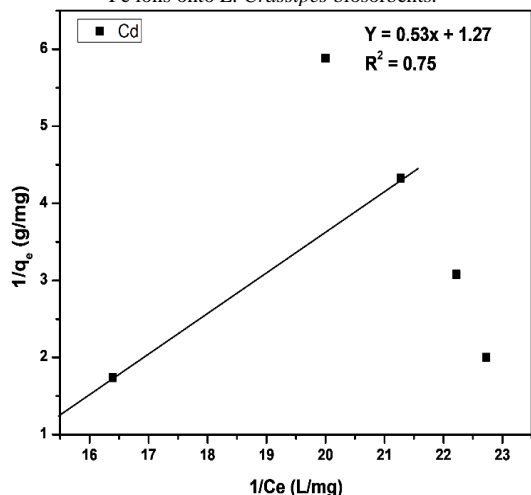


Fig 8e: Linear plots of Langmuir Isotherms for the adsorption of Cd metal ions onto *E. Crassipes* biosorbents.

Freundlich isotherm: Figure 9 presents the linear plots of the Freundlich model for the adsorption of the five metal ions investigated in this study. The various parameters as deduced from the plots of $\ln q_e$ against $\ln C_e$ are presented in Table 2.

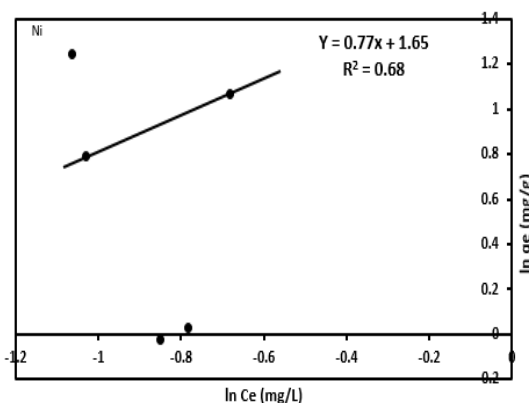


Fig 9a: Linear plots of Freundlich Isotherms for the adsorption of Ni metal ions onto *E. Crassipes* biosorbents

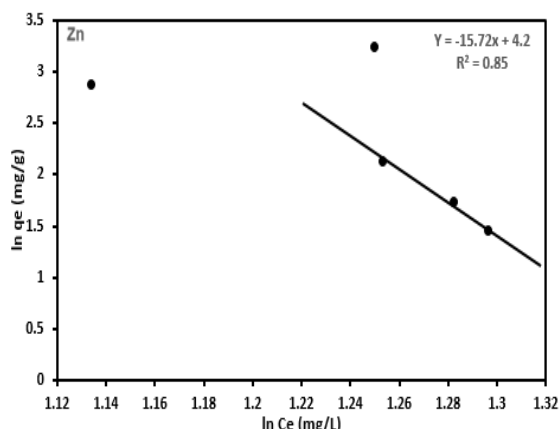


Fig 9b: Linear plots of Freundlich Isotherms for the adsorption of Zn metal ions onto *E. Crassipes* biosorbents

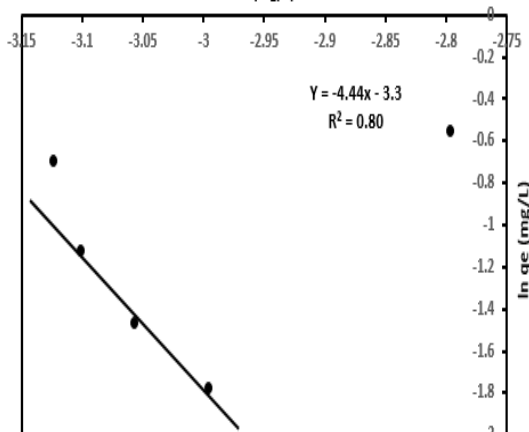


Fig 9: Linear plots of Freundlich Isotherms for the adsorption of Cd metal ions onto *E. Crassipes* biosorbents

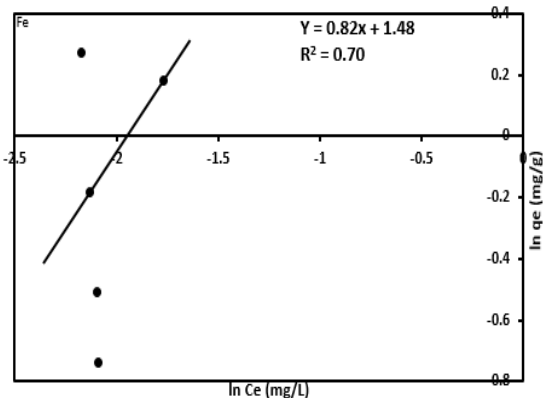


Fig 9: Linear plots of Freundlich Isotherms for the adsorption of Fe metal ions onto *E. Crassipes* biosorbents

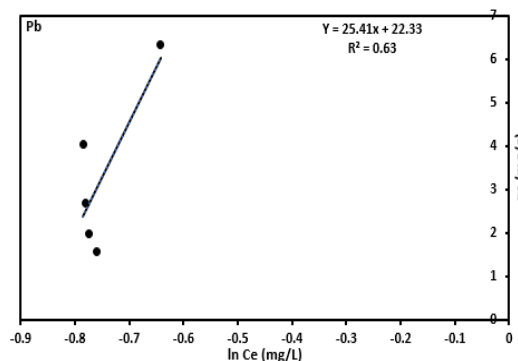


Fig 10b: Linear plots of Temkin Isotherms for the adsorption of Pb metal ions onto *E. crassipes* biosorbents

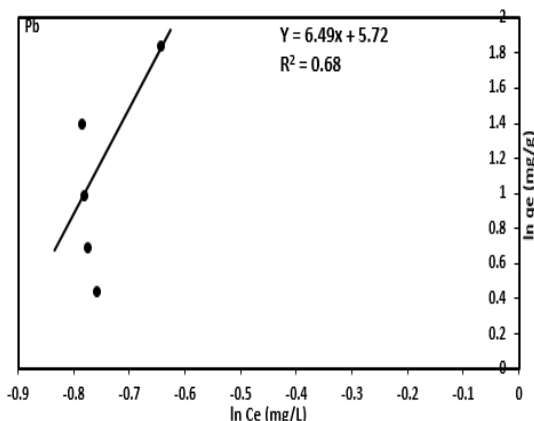


Fig 9e: Linear plots of Freundlich Isotherms for the adsorption of Pb metal ions onto *E. Crassipes* biosorbents

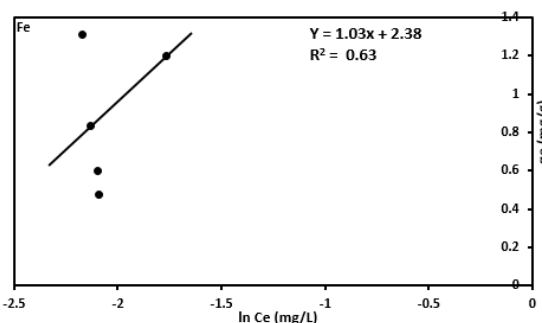


Fig 10c: Linear plots of Temkin Isotherms for the adsorption of Fe metal ions onto *E. crassipes* biosorbents

Temkin isotherm: Table 2 shows the values for Temkin constant related to the heat of adsorption in Joules per mol (b), equilibrium binding constant (K_T), and correlation coefficient (R^2) as derived from Figure 10 linearize plot q_e against $\ln C_e$ for Cd, Pb, Fe, Zn and Ni metal ions.

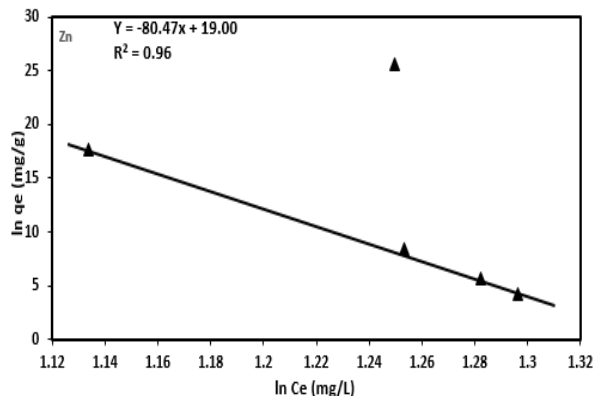


Fig 10d: Linear plots of Temkin Isotherms for the adsorption of Zn metal ions onto *E. crassipes* biosorbents

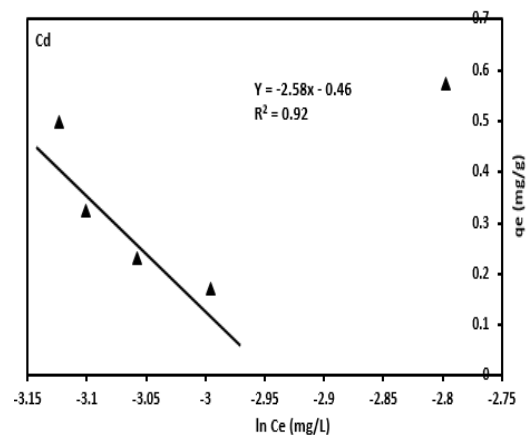


Fig 10a: Linear plots of Temkin Isotherms for the adsorption of Cd, metal ions onto *E. crassipes* biosorbents

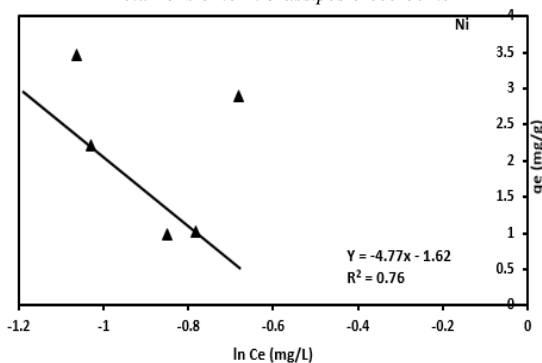


Fig 10e: Linear plots of Temkin Isotherms for the adsorption of Ni metal ions onto *E. crassipes* biosorbents

Freundlich equilibrium constants were determined from the plot of $\ln q_e$ against $\ln C_e$ from Figure 9 on the basis of the linear form of Freundlich equation. The n value in Freundlich equation was found to be from -0.23 - 1.3 (Table 2). The situation $n > 1$ is most common and may be due to a distribution of surface sites or any factor that causes a decrease in adsorbent-adsorbate interaction with increasing surface density (Mulu, 2013) and the values of n within the range 1-10 represent good adsorption (Mulu, 2013). In the present study, since n lies approximately between 0 and 1, it indicates the favourable adsorption of metal ion onto water hyacinth (*E. Crassipes*). The Temkin adsorption model was chosen to evaluate the adsorption potentials of the adsorbent. The plots for the five (5) metal ions are presented in Figure 10 and the isotherm parameters are given in Table 2. The Temkin adsorption potentials (K_T) of *E. Crassipes* biomass for Nickel, zinc Iron, Lead and Cadmium shows a higher adsorption affinity for Cadmium ion followed by Iron and then the least, zinc ion.

Table 2: Parameters deduced from the plot of Langmuir, Freundlich and Temkin isotherms for Pb, Cd, Zn, Fe and Ni metal ions adsorption onto *E. Crassipes* biosorbents

Freundlich isotherm	R ²	n	K _f [(mg/g)(mg/L) ^{1/n}]
Pb	0.68	0.15	658.53
Cd	0.80	-0.23	0.04
Zn	0.85	-0.06	66.67
Fe	0.70	1.22	4.39
Ni	0.68	1.30	5.21
Langmuir isotherm	R ²	b (L/mg)	q _m (mg/g)
Pb	0.78	0.08	8.33
Cd	0.75	2.40	0.79
Zn	0.82	-0.05	2.38
Fe	0.78	1.27	1.43
Ni	0.82	-1.46	0.81
Temkin isotherm	R ²	b _T (KJ.mol ⁻¹)	k _T
Pb	0.63	89.32	2.41
Cd	0.92	-4,934.18	273.14
Zn	0.96	119.46	0.01
Fe	0.63	2,203.61	10.07
Ni	0.76	-475.83	1.40

The basic assumption of the Langmuir isotherm is based on monolayer adsorption of the adsorbates on the surface of adsorbent (Nadeem *et al.*, 2006). This indicates that the adsorption of Fe, Ni and Pb ions onto the *E. Crassipes* biosorbents generates monolayer formation.

Conclusion: This study set out to investigate the effectiveness of Water Hyacinth extract in removing heavy metals from ALEX effluents. Optimal percentage removal of the metal occurred at 30 minutes except for Cd ions. Langmuir model had a better fit for Fe, Ni and Pb ions while Temkin model were best for Cd and Zn ions in the biosorption process. Water hyacinth could, therefore, serve as an efficient and cost-effective biosorbents for treating

heavy metal contaminated wastewater before discharging to the environment.

Table 2 presents the Temkin constants, b_T , related to the heat of adsorption. Ho *et al.* (1995) reported that the typical range of bonding energy for the ion exchange mechanism is 8.0 - 6.0 KJ/mol. Nickel and Cadmium showed low values in this study indicating a weak interaction between the adsorbent and adsorbate, supporting an ion exchange mechanism. To find the most appropriate model for the metal ions adsorption, data were fitted to Langmuir, Freundlich, and Temkin Isotherm models. The results revealed that Langmuir model had a better fit for Fe ($R^2 = 0.78$), Ni ($R^2 = 0.82$) and Pb ($R^2 = 0.78$), while Temkin model fitted best for Cd ($R^2 = 0.92$) and Zn ($R^2 = 0.96$) unto the Water Hyacinth biosorbent. The R^2 values for the Fe, Ni and Pb from Langmuir isotherm shows the low efficiency in the adsorption capacity of the biosorbents. This points to the need for further chemical treatment of the sorbent material for increased adsorption efficiency.

heavy metal contaminated wastewater before discharging to the environment.

REFERENCES

- Abechi, SE; Gimba, CE; Uzairu, A; Dallatu, YA (2013). Preparation and characterization of activated carbon from palm kernel shell by chemical activation. *Res. J. Chem. Sci.* 3(7): 54-61.
- Akinyemiju, OA (1987). Invasion of Nigerian waters by water hyacinth. *J. Aquatic Plant Manage.* 25: 24-26.
- Ali, AA-H; Haeel, JA-H; Amal, AA-H; Gehan, E Nadine, MSM (2014). Biosorption of Copper ions

- from aqueous solution by *spirulina platensis* biomass. *Arab. J. Chem.* 7(1): 57-62.
- Ali, HR; Hassaan, MA (2017). Applications of biowaste materials as green synthesis of nanoparticles and water purification. *Adv. Mater. Che.* 1(1): 6-22.
- Genoveva, GR; Olguin, MT; Colin-cruz, A; Guzman, ER (2014). Effect of the pH and Temperature on the biosorption of Lead (II) and Cadmium (II) by sodium modified stalk spong of *Zea mays*. *Environ. Sci. Pollut. Res.* 19(1): 177-185.
- Gunatilake, SK (2015). Methods of removing heavy metals from industrial wastewater. *J. Multid. Eng. Sci. Stud.* 1(1): 2912-1309.
- Guyo, U; Moyo, M (2017). Cowpea pod (*Vigna unguiculata*) biomass as a low-cost biosorbent for removal of Pb (II) ions from aqueous solution. *Environ. Monitor. Ass.* 189, 47-59.
- He, Z; Shentu, T; Yang, X; Baligar, VC; Zhang, T; Stoffella, PJ (2015). Heavy metal contamination of soils: Sources, indicators, and assessment. *J. Environ. Indi.* 9:17-18.
- Ho, YS; McKay, G (1998): A comparison of chemisorption kinetic models applied to pollutant removal on various sorbents. *Pro. Safe. Environ. Protect.* 76: 332-340.
- Horsfall, M Jnr; Eyitemi, EA (2006). Recovery of Lead and Cadmium ions from metal-loaded biomass of wild Cocoyam (*Caladium bicolor*) using acidic, basic and neutral eluent solution. *Elect. J. Biotech.* 9(2): 153-155.
- Horsfall, M Jnr; Spiff, A I (2005). Effects of temperature on the sorption of Pb²⁺ and Cd²⁺ from aqueous solution by *caladium bicolor* (wild cocoyam) biomass. *Elect. J. Biotech.* 8(2).
- Mahamadi, C (2011). Water Hyacinth as a biosorbent: A review: *Afr. J. Environ. Sci. Technol.* 5(13): 1137-1145.
- Mahamadi, C; Nharingo, T (2007). Modelling the kinetics and equilibrium properties of Cadmium bio-sorption by River green alga and water hyacinth weed. *Tox. Environ. Che.* 89(2): 297-305.
- Mahamadi, C; Nharingo, T (2010). Utilization of water hyacinth weed (*Eichhornia crassipes*) for the removal of Pb(II), Cd(II) and Zn(II) from aquatic environment: an adsorption Isotherm study. *Environ. Technol.* 31(11): 221-1228.
- Mulu, BD (2013). Batch sorption experiments: Langmuir and Freundlich Isotherm studies for the adsorption of textile metal ion onto Teff straw (*Eragrostis tef*) agricultural waste. *J. Thermo.* 375830: 1-6.
- Munene, JM; Onyatta, JO; Yusuf, AO (2020). Characterization of water hyacinth powder using FTIR spectroscopy and the adsorption behaviour of Pb²⁺, Cd²⁺, Zn²⁺, Ni²⁺ and Cr²⁺ in Aqueous Solution. *Asian J. Appl. Che. Res.* 6(1): 47-55.
- Nadeem, M; Mahmood, A; Shahid, SA; Shah, SS; Khalid, AM; McKay, G (2006). Sorption of lead from aqueous solution by chemically modified carbon adsorbents. *J. Hazar. Mater.* 138: 604-613.
- Nwoko, CO; Okwara, I; Ihejirika, CE; Nwosu, OU (2016). Biosorption of Pb(II) and Ag (I) from pulp and paper mill effluent using corn cob (*Zea mays*) and plantain bunch stalk (*musa paradisiaca*). *J. Environ. Sci. Pollut. Res.* 2(3): 95-98.
- Onwordi, CT; Uche, CC; Ameh, AE; Petrik, LF (2019). Comparative study of the adsorption capacity of lead (II) ions onto bean husk and fish scale from aqueous solution. *J. Wat. Reuse Desal.* 9, 3: 249 – 262.
- Uka, UN; Chukwuka, KS; Daddy, F (2007). Water Hyacinth Infestation and Management in Nigeria inland waters: A Review. *J. Plant Sci.* 2: 480-488.
- Volesky, B (1990). Biosorption and Biosorbent. In: Heavy Metals. CRC Press Inc., Florida.